

Synthesis and SAED Investigation of a Misfit-Layered Magnesium Hydroxide Manganese Oxide

Yaohua Xu¹, Noriaki Nakayama*, Keiko Fujiwara, Tadato Mizota, and Seishi Goto

Department of Advanced Materials Science and Engineering, Faculty of Engineering, Yamaguchi University, Ube 755-8611, Japan

Fax: 81-836-85-9601, e-mail: nakayamn@yamaguchi-u.ac.jp

New layered magnesium hydroxide manganese oxides (MHMO) with $d \sim 10$ Å have been hydrothermally synthesized by using birnessite as the precursor. The selected-area electron diffraction (SAED) analysis indicates that these compounds have noncommensurate layered structures composed of two pseudo-hexagonal sublattices; namely, MnO_2 -type and $\text{Mg}(\text{OH})_2$ -type mono-atomic layers are stacked alternately with a small in-plane lattice misfit. One of these misfit layered compounds has a chemical formula of $[\text{Mg}(\text{OH})_2]_{10}[\text{MnO}_{1.86}(\text{OH})_{0.07}]_{14} \cdot 2.34\text{H}_2\text{O}$. The actual symmetry of each sublattice is monoclinic. The lattice parameters of the monoclinic MnO_2 sublattice are $a_1=0.496(2)$ nm, $b_1=0.292(5)$ nm, $c_1=0.957(2)$ nm and $\beta_1=94.1(9)^\circ$, whereas, those for the monoclinic $\text{Mg}(\text{OH})_2$ sublattice are $a_2=0.534(6)$ nm, $b_2=0.313(6)$ nm, $c_2=0.958(1)$ nm and $\beta_2=94.8(4)^\circ$. The mutual relationships of two sublattices are $(001)_1 // (001)_2$, $\mathbf{a}_1 // \mathbf{a}_2$ and $\mathbf{b}_1 // \mathbf{b}_2$. TG-DTA analyses show that this misfit-layered hydroxide oxide can be stable up to 300°C .

Keywords: Hydrothermal synthesis, misfit-layered compound, Manganese oxide, Magnesium hydroxide, Birnessite.

1. INTRODUCTION

Misfit-layered compounds are very interesting due to their unusual structures as well as their properties.[1-5] In the misfit-layered cobalt oxide, $[\text{M}_m\text{A}_2\text{O}_{2+m}]_q\text{CoO}_2$ with $m=1$ or 2 , $\text{M}=\text{Co}$, Bi , etc. and $\text{A}=\text{Ca}$, Sr , etc., the hexagonal CoO_2 layers are coupled incoherently with square-planar metal oxide layers, and the incommensurate mismatch is formed along one of the two in-layer crystal axes, the b-axis. The "misfit parameter" q can be determined by the ratio of the mutually incommensurate b-axes of the two subsystems. The further investigation in the misfit-layered cobalt oxide showed that there must occur considerable amounts of oxygen vacancies in at least one of the three types of layers, CoO , CaO and CoO_2 in the samples synthesized in air or in a more reducing atmosphere.[6] A general feature for another misfit-layered compounds $(\text{MS})_n\text{TS}_2$ with $\text{M}=\text{Sn}$, Pb , Bi and La and $\text{T}=\text{Nb}$, Ta , V , Cr and Ti is that the lattices have a common (b^*, c^*) -plane.[7] Although there are several different possibilities for the combinations of intra-layer axes for the two subsystems in misfit-layered compounds with c^* common, however, only one of them has been found in the real compound. There are many kinds of mixed layered compounds in the nature.[8-11] Some of these mixed layered compounds have misfit-layered structures.[9,10] However, there are less attentions have been paid to them perhaps due to the facts that the misfit-layered crystals grown in the natural condition are always disordered in the layers stacking with poor crystallinity.

It is an attractive method to use layered compounds as precursors for the preparation of new compounds.[12-14] Birnessite, $\text{Na}_{4.1}\text{Mn}_{14}\text{O}_{27} \cdot 9\text{H}_2\text{O}$, is a kind of layered manganese oxide, and many compounds have been synthesized by using it as the precursor.[15-17] In this paper, we present a novel compound with a misfit layered structure composed of $\text{Mg}(\text{OH})_2$ and MnO_2 sublattices, which was hydrothermally synthesized from birnessite and has a layer spacing of about 0.95 nm.

2. EXPERIMENTAL SECTION

Birnessite (Bir-A) was synthesized according to the method described in the literature.[18,19] In order to increase the crystallinity, Bir-A was further hydrothermally treated in 2 mol/L NaOH solution at 200°C for 10 hours. This birnessite was labeled as Bir-B. The magnesium hydroxide manganese oxide (MHMO) was synthesized as follows: Bir-B (wet) was dispersed into a solution of MgCl_2 , and the solution was stirred for 1 day, then a 0.5 mol/l NaOH solution was added into the solution until $\text{pH}=11-12$. After filtration and washing, the precipitate was autoclaved in water at 200°C for 1 – 3 days.

The metal element contents in the samples were determined by the polarized Zeeman atomic absorption spectrophotometer (Z-5310) as well as the energy-dispersive X-ray (EDX) spectroscopy analysis.

Powder X-ray diffraction (XRD) patterns of the samples were recorded on a X-ray diffractometer with $\text{Cu K}\alpha$ ($\lambda = 0.15418$ nm) radiation. Infrared spectra (IR) were measured with the KBr method on a

¹The venture business laboratory (VBL), Yamaguchi University, Ube 755-8611, Japan.
Current address: Department of Chemistry, Jilin University, Changchun 130010, China

HORIBA FT-IR infrared spectrometer. Thermogravimetric (TG) data and differential thermal analysis (DTA) curves were recorded at a heating rate of 10°C/min in air on a MacScience 2000S thermal analyzer. Transmission electron microscope (TEM) observation, selected-area electron diffraction (SAED) and EDX investigations were carried out on a field emission type TEM (JEOL JEM2010F) operated at 200kV.

3. RESULTS AND DISCUSSION

Fig. 1 shows XRD patterns of birnessite precursors. Bir-A was prepared by the conventional method. The crystallinity is very poor although the aging time was longer than 20 days. Bir-B was obtained by hydrothermally treating of Bir-A in NaOH solution. The crystallinity is greatly increased as shown in Fig.1(b). Na^+ ions in Bir-A are easily ion-exchanged with Mg^{2+} ions. However, Na^+ ions in Bir-B are very difficult to be exchanged. In fact, after 5 days ion-exchange in MgCl_2 solution, XRD pattern of Bir-B did not change (sample A), and after more than 2 months ion-exchange, Bir-B was transformed to a mixture of birnessite and Mg-Bir (sample B).

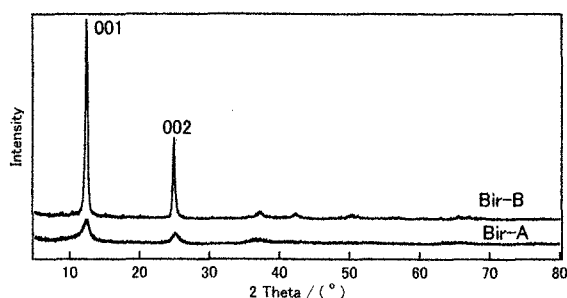


Fig. 1. XRD patterns of birnessite precursors; pristine (Bir-A) and hydrothermally treated (Bir-B) samples

Fig. 2 shows the XRD of products prepared by hydrothermal synthesis from the birnessite precursor which was firstly ion-exchanged in MgCl_2 solution. Sample C was prepared with the sample A as the precursor. It is a mixture of birnessite and magnesium hydroxide manganese oxide (MHMO) (Fig. 2A). Sample D was prepared with the sample B as the precursor, and sample E is the product of the sample D after hydrothermal treatment. The samples D and E are still the mixture of birnessite and MHMO (Fig. 2B and C), although the amount of birnessite became less.

Fig. 3 shows the products hydrothermally prepared from birnessite. In this preparation, during the ion-exchange, NaOH solution was added till the pH value is about 12. For sample F, the molar ratio of Mn/Mg is about 1.5 in the starting materials. For sample G, the molar ratio of Mn/Mg is about 1. Both of them have similar XRD patterns with two main peaks at low degree. This indicates that the pure MHMO can be synthesized by this way. However, in the IR spectrum of sample G there is a sharp peak at 3698 cm^{-1} , indicating that the sample G contains a little $\text{Mg}(\text{OH})_2$.

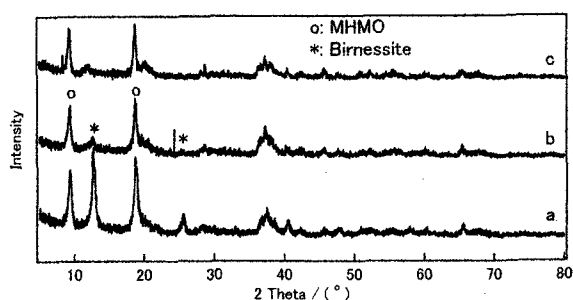


Fig. 2. XRD patterns of Mg-exchanged birnessites; (a) sample C from Bir-A, (b) sample D from Bir-B and (c) sample D hydrothermally treated (sample E)

So the amount of $\text{Mg}(\text{OH})_2$ in the starting material has a limitation for the synthesis of MHMO.

The main two peaks in the XRD pattern of MHMO are at 0.95 nm and 0.48 nm, and can be indexed as 001 and 002, respectively. The 001 peak is lower than the 002 peak, indicating that there are less opening between the (001) layers. These d spacing are very similar to that of the busserite and todorokite [15,20], which also have two main peaks in their XRD patterns. Busserite is a layered compound. There are more open space between the MnO_2 layers, so the first peak nearby $d = 0.95\text{ nm}$ is higher than the second peak nearby $d = 0.48\text{ nm}$ in the XRD pattern. Todorokite has a 3×3 tunnel structure. There are less opening among the MnO_2 layers, and the first peak nearby $d = 0.95\text{ nm}$ is lower than that nearby $d = 0.48\text{ nm}$ in the XRD pattern. The XRD pattern of MHMO (Fig. 3) is too similar to that of todorokite, and the peaks at high degree are too weak to be indexed. (Fig. 3c). So it is very difficult to determine the structure of this MHMO compound is either layered or tunnel only based on the XRD analysis. So we have carefully investigated this MHMO compound (sample F) with TEM and SAED analyses.

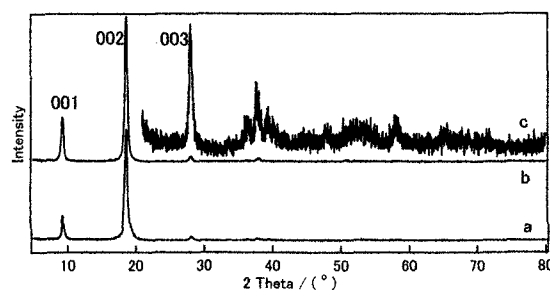


Fig. 3. XRD patterns of MHMO prepared by adding NaOH solution during the ion exchange; Mn/Mg molar ratios are (a) about 1 (plot a, sample F) and (b) 1.5 (plots b and c, sample G), respectively

TEM images of sample F show that the most of MHMO are large sheet-like crystals with two kinds of appearances; ones are the smaller pseudo-hexagonal sheet crystals with the diameters ranging from 800 to 200 nm, and the others are rectangular sheet crystals with the dimensions ranging from 7000×3000 to

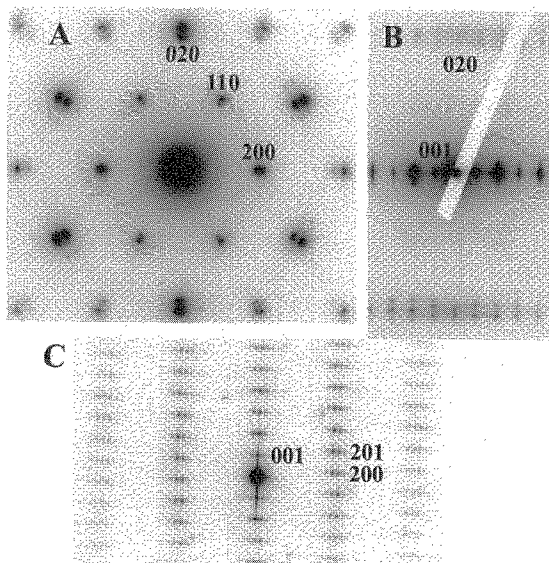


Fig. 4. The SAED patterns of sample F. (A) of the big sheet-like crystal, (B) and (C) of the thin and stick-like crystals.

1000×150 nm, which appearance is similar to that of the precursor Bir-B. However, both of these two kinds of sheet crystals show the same SAED pattern as shown in Fig. 4A and the similar EDX spectra, suggesting that these crystals have the same composition and crystal structure. Besides the sheet-like crystals, a few of the crystals are thin and stick-like with the typical dimension of 600×30 nm and give the SAED patterns similar to either Fig. 4B or 4C. The EDX spectra also show that these crystals have the same composition as that of the sheet-like crystals. The observed longest lattice spacing in the SAED patterns in Fig. 4B and C, $d=0.97$ nm, agrees with the lattice spacing of the first peak in the XRD pattern, $d=0.954$ nm, and the d spacings observed in Fig. 4A are in agreement with those of the very weak peaks found in the XRD pattern. The high-resolution transmission electron microscopy images of the stick-like crystals also show almost regular lattice fringes of about 0.95 nm (Fig. 5).

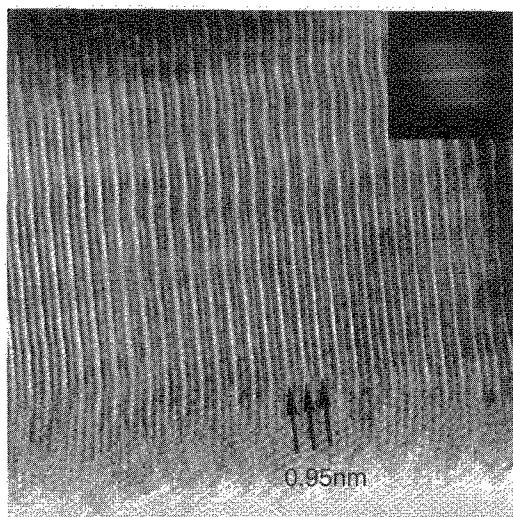


Fig. 5. A lattice image of sample F showing the layer stacking of about 0.95 nm.

Fig. 4A shows that the spots have a pseudo-hexagonal symmetry and the pattern is similar to the [001] zone SAED pattern of the monoclinic birnessite-type structure ($C2/m$). [21] However, each diffraction spot splits into two or more spots; for example, $d_1=0.148$ nm and $d_2=0.159$ nm for two intense spots corresponding to the 020 reflection. The shorter d_1 almost agrees with the 020 lattice spacing (0.142 nm) of the birnessite. [21] The longer d_2 almost agrees with the $d(110)=0.153$ nm of hexagonal ($P\bar{3}m$) $Mg(OH)_2$. [22] The spots in the SAED patterns in Fig. 4B and C can be indexed as [010] and [100] zone diffraction patterns of $C2/m$ lattice, respectively. They also show the splitting for most of the diffraction spots along a^* and b^* . However, they show no splitting along c^* axis, indicating the regular stacking of the layer units.

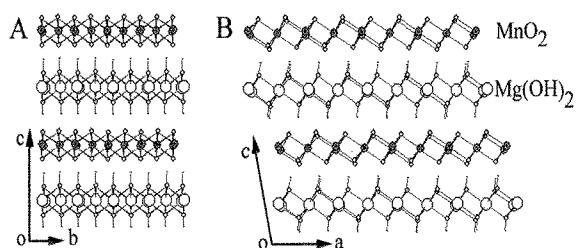


Fig. 6. The proposed structure of the misfit-layered MHMO.

Table I. The lattice parameters and the proposed atomic positions as the ideal space group of $C2/m$ model of MHMO

Lattices	a	p	p.o. .f	x	y	z
Lattice I, $a_1=0.496(2)$ nm $b_1=0.292(5)$ nm $c_1=0.957(2)$ nm, $\beta_1=94.1(9)^\circ$	Mn	2a	1	0	0	0
	O	4i	1	0.352	0	0.109
Lattice II, $a_2=0.534(6)$ nm $b_2=0.313(6)$ nm $c_2=0.958(1)$ nm $\beta_2=94.8(4)^\circ$	Mg	2a	1	0	0	0.5
	O	4i	1	0.646	0	0.382
	H	4i	1	0.646	0	0.283

The above features of SAED patterns indicate that the present MHMO has a layered structure built with non-commensurate sheets of MnO_2 and $Mg(OH)_2$ as shown in Fig. 6. This model structure is based on the commensurate structure reported for lithiophorite $[(Al,Li)MnO_2(OH)_2]$ in which the octahedral (or CdI_2 -type) MnO_2 and $(Al,Li)(OH)_2$ sheets are stacked alternately. [23] Assuming the space group $C2/m$ for both MnO_2 and $Mg(OH)_2$ sublattices (sublattice I and II, respectively), the lattice parameters of two sublattices have been deduced from SAED and XRD patterns as listed in Table 1. The probable atomic positions are also listed in the Table 1. The mutual relationship of the two sublattices is that $c_1=c_2$, and b_1^*/b_2^* in the reciprocal space. In the real space, $d_{(001)}=c_1\sin\beta_1=c_2\sin\beta_2$, a_1/a_2 and b_1/b_2 . The two sublattices are non-commensurate both along the

lateral a and b axes, and the β angles are also different. This misfit-layered structure is different from the most of the reported misfit layered structure, which is non-commensurate only along the one direction and the two sublattices have different in-plane symmetry.

The compositions of Mn, Mg and Na for sample F analyzed by AAS are 34.5%, 10.8% and 0.01% in mass, respectively. The molar ratio of Mn/Mg is 1.41. The EDX analysis shows that there is no sodium and the Mn/Mg molar ratio is about 1.3~1.4, which is in agreement with the AAS result. Taking the water contents estimated from TG measurements into account, the chemical formula of sample F is $[\text{Mg}(\text{OH})_2]_{10}[\text{MnO}_{1.86}(\text{OH})_{0.07}]_{14} \cdot 2.34\text{H}_2\text{O}$. The molar ratio of Mn/Mg is 1.16 calculated according to the ideal model structure in Fig. 6, and is smaller than that obtained from the AAS analysis (Mn/Mg=1.41). Some vacancies and/or the incorporation of manganese atoms in the $\text{Mg}(\text{OH})_2$ sublattices are well assumed as the origin of the discrepancy. For example, without any vacancies, replacement of 10 at.% of Mg atoms with Mn atoms in the $\text{Mg}(\text{OH})_2$ sublattice will give the Mn/Mg=1.4 in molar ratio in the MHMO.

Fig. 7 shows the TG-DTA curves of sample F. The endothermic peak at 42°C in the DTA curve and 2.3% weight loss between 25°C and 300°C in TG curve are attributed to the loss of water absorbed by the compound. The endothermic peak at 390°C in the DTA curve and 10.3% weight loss between 300°C and 550°C in the TG curve are ascribed to the water loss resulted from the decomposition of metal hydroxide of the sample. The sharp endothermic peak at 656°C in the DTA curve and 4.9% weight loss between 550°C and 700°C in the TG curve are preferred to the evolution of O_2 . The XRD analyses show that this misfit-layered hydroxide oxide is stable up to 300°C. The compound is transformed to MgMn_2O_4 -like compound after calcinations at 1000°C.

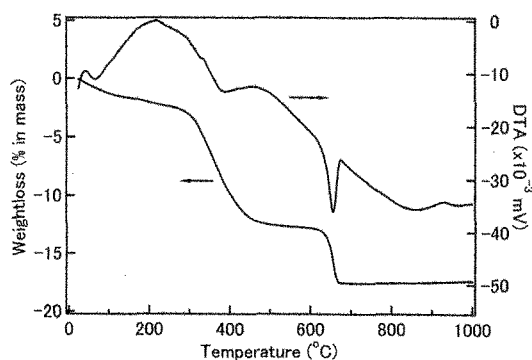


Fig. 7. TG-DTA curves of sample F

4. SUMMARY

The crystallinity of birnessite synthesized with the common method is usually very low. After a further hydrothermal treatment in NaOH solution at 200°C, the crystallinity of the birnessite is greatly increased. A misfit-layered magnesium hydroxide manganese oxide has been hydrothermally synthesized by using the birnessite with high crystallinity. The formation of MHMO is a topotactic reaction in which the MnO_2 layers of birnessite are kept. It is reasonable expected that this synthesis method can be applied to the

synthesis of other layered compounds, and this misfit-layered compound can be used as a precursor for a synthesis of some novel compounds.

Acknowledgement

We thank the venture business laboratory (VBL) for the support to this research.

References

- [1] J. Morales, J. Santos, J. Baas, G. A. Wieggers and J. L. Martinez, *Chem. Mater.*, 1999, **11**(10), 2737.
- [2] I. Terasaki, Y. Sasago and K. Uchinokura, *Phys. Rev. B*, 1997, **56**, R12685.
- [3] S. Li, R. Funahashi, I. Matsubara, K. Ueno and H. Yamada, *J. Mater. Chem.*, 1999, **9**, 1659.
- [4] S. Hebert, S. Lambert, D. Pelloquin and A. Maignan, *Phys. Rev. B*, 2001, **64**, 172101.
- [5] O. Pena, P. Rabu and A. Meerschaut, *J. Phys.: Condens. Matter.*, 1991, **3**, 9929.
- [6] M. Karppinen, H. Fjellvag, T. Konno, Y. Morita, T. Motohashi and H. Yamauchi, *Chem. Mater.*, 2004, **16**, 2790.
- [7] G. A. Wieggers, A. Meetsma, S. van Smaalen, R. J. Haange and J. L. de Boer, *Solid State Commun.*, 1990, **75**(9), 689.
- [8] J. E. Post and D. E. Appleman, *Am. Mineral.*, 1994, **79**, 370.
- [9] D. Schmidt and K. J. T. Livi, *Am. Mineral.*, 1999, **84**, 160.
- [10] A. Manceau, A. I. Gorshkov and V. A. Drits, *Am. Mineral.*, 1992, **77**, 1144.
- [11] F. V. Chukhrov, B. A. Sakharov, A. I. Gorshkov, V. A. Drits and Y. P. Dikov, *Inter. Geo. Rev.*, 1985, **27**, 1082.
- [12] J.-H. Choy, S.-R. Lee, M. Park and G.-S. Park, *Chem. Mater.*, 2004, **16**, 3206.
- [13] D. Mochizuki, A. Shimojima and K. Kuroda, *J. Am. Chem. Soc.*, 2002, **124**, 12082.
- [14] R. E. Schaak and T. E. Mallouk, *Chem. Commun.*, 2002, 706.
- [15] D. C. Golden, C. C. Chen and J. B. Dixon, *Science*, 1986, **231**, 717.
- [16] Z. Liu and K. Ooi, *Chem. Mater.*, 2003, **15**, 3696.
- [17] Y. Xu, Q. Feng, K. Kajiyoshi and K. Yanagisawa, *Chem. Mater.*, 2002, **14**, 697.
- [18] Q. Feng, K. Yanagisawa and N. Yamasaki, *J. Porous. Mater.*, 1998, **5**, 154.
- [19] Y. Xu, Q. Feng, K. Kajiyoshi, K. Yanagisawa, X. Yang, Y. Makita, S. Kasaishi and K. Ooi, *Chem. Mater.*, 2002, **14**, 3844.
- [20] E. Vilenko, Y. Ma, H. Zhou and S. L. Suib, *Micro. Meso. Mater.*, 1998, **20**, 3.
- [21] V. A. Drits, E. Silvester, A. I. Gorshkov and A. Manceau, *Am. Mineral.* 1997, **82**(9-10), 946.
- [22] L. Desgranges, G. Calvarin and G. Chevrier, *Acta Cryst. B*, 1996, **52**, 82.
- [23] L. Pauling and B. Kamb, *Am. Mineral.* 1982, **67**(7-8), 817.

(Received December 24, 2004; Accepted April 23, 2005)